Journal of
Ceramic Science
and Technology

J. Ceram. Sci. Technol., **09** [3] 225-234 (2018)
DOI: 10.4416/JCST2018-00008
available online at: http://www.ceramic-science.com

Surface Modification of Alumina Powder to Prevent Exfoliation of Samples Fabricated by Gelcasting

A. Wieclaw-Midor*, P. Wiecinska, M. Szafran

Warsaw University of Technology, Faculty of Chemistry, 3 Noakowskiego Street, 00 – 664 Warsaw, Poland
received January 31, 2018; received in revised form April 4, 2018; accepted April 28, 2018

Abstract

The aim of this work was to study the influence of the Al_2O_3 surface modification 2-hydroxyethyl acrylate (HEA) on the properties of green and sintered ceramic bodies. As a reference, non-modified Al_2O_3 was used in the research. The modified Al_2O_3 powder was characterized with TEM and thermal analysis coupled with mass spectrometry. The rheological behaviour of slurries containing modified and non-modified alumina powder was measured, as well as the properties of green bodies. The proposed surface modification enables the production of green ceramic samples with homogeneous microstructure, high mechanical strength and high density. Sintered materials presented high density and favourable values for Vickers hardness. The obtained results showed that the presence of HEA on the powder surface partially prevents the negative effect of oxygen inhibition during gelcasting of alumina. Oxygen inhibition is a well-known problem in gelcasting but has still not been fully overcome for samples formed in an air atmosphere.

Keywords: Gelcasting, surface modification, alumina, mechanical strength

I. Introduction

Nowadays, shaping of ceramics has become more and more demanding to meet the needs of science and technology. It is desirable to produce materials with complex geometries, short moulding time and small quantities of environmentally friendly and water-soluble organic compounds. Furthermore, to fabricate new products with novel and unusual properties, various powders for example: Al_2O_3 [1,2], ZrO_2 [3,4], SiC [5,6], ZnO [7,8], Si_3N_4 [9,10], $BaTiO_3$ [11] have been examined to ascertain their behaviour during different compaction techniques. In this context, a large number of novel shaping methods based on colloidal processing has been developed [12]. Of the colloidal shaping techniques for alumina powder, the most popular seem to be: gelcasting [13,14], tape casting [15,16], direct coagulation casting [17,18] and slip casting [19,20]. These methods allow the production of thick or thin [21], dense [22] or porous [23,24] alumina materials. Alumina is the most commonly used engineering ceramic material, owing to its unique combination of high hardness, good mechanical strength and high density.

Gelcasting involves conducting *in-situ* polymerization which occurs in a ceramic slurry and, as a result, a macromolecular polymeric network is formed which connects the ceramic particles. The main challenge in this method is to obtain stable, homogeneous suspension with high solid loading. The selection of appropriate amounts of organic additives such as monomer, dispersing agent, activator or initiator of radical polymerization is necessary to obtain slurries with favourable parameters. To meet the increased requirements for the protection of the environment, it is now important to look for low-toxic, inexpensive and water-soluble organic additives. For this reason, there is great interest in compounds such as saccharides, their derivatives and polysaccharides, for example: D-fructose [25], glucuronic acid [26], 3-O-acryloyl-D-glucose [27], agarose [28], which could play the role of deflocculants, monomers or gelling additives for suspensions containing alumina powder.

Gelcasting has many advantages, for example it is a near-net-shaping method with relatively short moulding time [29]. However, this technique has some disadvantages that hinder the use of gelcasting in industry for large-scale production. The main problems are: proper drying of large ceramic parts and the oxygen inhibition that appears during the shaping process. They lead to a decrease in the mechanical strength of the green bodies and the formation of various defects (e.g. surface exfoliation, microcracks). The research in this paper concerns oxygen inhibition and prevention of surface exfoliation of samples, and therefore this problem is described in greater detail.

In the gelcasting process, oxygen is a known inhibitor of radical polymerization. If chain propagation has started and oxygen molecules are present, the oxygen becomes attached to the growing chain, creating peroxide radicals that are inactive in the polymerization process. This mechanism has been explained more extensively elsewhere [30]. Oxygen inhibition unfavourably influences the quality of the polymeric network that holds the ceramic particles together. This problem can be partially mitigated, for example, by replacing the air atmosphere during casting with CO_2, N_2 or vacuum [31]. Furthermore, new monomers that are more resistant to oxygen are still required [32]. More-

* Corresponding author: awieclaw@ch.pw.edu.pl

over, it is desirable to obtain a stable suspension with favourable viscosity and homogeneous distribution of organic additives. The insufficient distribution of a small amount of organic additives causes the lack of perfect homogenization. As a result, gelation of obtained ceramic slurry does not occur in the total volume of the sample but only in some areas. Consequently, green bodies with low mechanical strength, microcracks and various deformations are obtained. Literature data shows that one possible method to change the properties of ceramic powders is surface modification. There are known modifications of alumina powder with 1,6-hexanediol diacrylate and its application in the preparation of UV-curable ceramic suspensions [33] or stearic acid to improve the rheological properties [34]. In this work, the influence of surface modification of alumina powder based on the impregnation method and 2-hydroxyethyl acrylate (HEA) on the rheological characterization of slurries and selected properties of obtained samples was examined. Additionally, the possible impact of the presence of HEA on the powder surface on the limitation of oxygen inhibition and surface exfoliation of green bodies has been studied. The results for modified alumina powder were compared with the results for non-modified alumina.

II. Experimental

(1) Materials

The ceramic powder used in the research was α-Al_2O_3 TM-DAR (Tamei Chemicals, Japan) with an average particle size of 115 nm and a specific surface area 12.98 m^2/g measured on an ASAP 2020 V3.01 (Micromeritics, USA). The density of the powder was 4.02 g/cm^3 measured on an AccuPyc 1340 Pycnometer (Micromeritics, USA). In this paper, abbreviated names of powders are used as follows: for non-modified powder – non-m-Al_2O_3 and for modified powder – m-Al_2O_3. To obtain samples with the gelcasting method, additional organic additives have been used. Diammonium hydrocitrate, DAC (pure, POCh, Poland) and citric acid, CA (99.5 %, Sigma-Aldrich) were used as dispersing agents for the ceramic particles in the slurries. Commercially available 2-hydroxyethyl acrylate, HEA (96 %, Sigma-Aldrich) was used as the monomer (for non-modified powder) and as impregnating agent (for modified powder). N,N,N',N'-tetramethylethylenediamine, TEMED (98 %, Fluka) and ammonium persulfate, APS (98 %, Sigma-Aldrich) were used as an activator and an initiator of polymerization, respectively. The suspensions were prepared in Milli-Q deionized water.

(2) Modification of powder; slurries and sample preparation

The first step was the preparation of alumina powder with modified surface by using 2-hydroxyethyl acrylate. The scheme of this process is shown in Fig. 1. Alumina powder was dispersed in 2-hydroxyethyl acrylate with mass ratio 5:4. The suspension was stirred with a magnetic stirrer for 6 h at a speed of 400 rpm and kept at room temperature for 24 h. Then the suspension was centrifuged at 10 000 rpm for 10 min in an MPW-350R High-Speed Brushless Centrifuge, MPW Med. Instruments. The centrifuged powder was dried at 50 °C for 24 h and homogenized in an agate mortar. Samples based on non-m-Al_2O_3 and m-Al_2O_3 were prepared in a gelcasting process, shown schematically in Fig. 1.

Three types of ceramic slurries (A – with non-m-Al_2O_3, B – with m-Al_2O_3 and C – containing the mixture of A and B) were first prepared in alumina containers. Dispersing agents were dissolved in deionized water followed by HEA in slurry A. In the case of slurries B and C, HEA was not added because the monomer was already present on the surface of the modified powder. Then the appropriate amounts of ceramic powder (non-m-Al_2O_3 or m-Al_2O_3) were dispersed and the polymerization activator was added. The slurries were mixed in a planetary ball mill (PM-200, Retsch) for 60 min at a speed of 300 rpm. The suspensions were then mixed and degassed in a Planetary Centrifugal Mixer THINKY ARE-250 for 2 x 4 minutes at a speed of 800 rpm (mixing) and 1800 rpm (degassing) to remove bubbles > 1 μm. In the next step, the initiator was added to initiate the *in-situ* polymerization, then mixing and degassing were performed for 2 x 30 s at a speed of 800 rpm (mixing) and 1800 rpm (degassing). The prepared slurries with favourable viscosity (A and C) were cast into PVC moulds with a diameter measuring 20 mm and a height of 10 mm, where polymerization continued. The obtained green bodies after gelation were removed from the moulds and dried for 24 h at room temperature. Then the specimens were polished with SiC abrasive papers with gradation in the range from P500 to P1500 to smooth the surface prior to mechanical strength measurement.

The samples were sintered at 1400 °C/1 h, the heating rate up to 600 °C was 1 K/min, and then 5 K/min up to 1400 °C. The cooling rate was 5 K/min down to room temperature. The concentrations of all components are listed in Table 1.

(3) Characterization techniques

The densities of non-m-Al_2O_3 and m-Al_2O_3 powders were measured with an AccuPyc 1340 Pycnometer (Micromeritics, USA). The microstructure of the modified powder was examined under a transmission electron microscope (FE-SEM Hitachi S5500). Selected thermal analysis techniques were used. Thermogravimetry (TG), derivative thermogravimetry (DTG) and differential thermal analysis (DTA) were performed using a Netzsch STA 449C coupled with a Quadrupole Mass Spectrometer (MS) Netzsch QMS403C.

The temperature was varied from 35 °C to 1000 °C; the heating rate was 5 K/min. The measurements were performed in the constant flow of two gases: argon – 10 ml min^{-1} (protective gas) and synthetic air (75:25 N_2:O_2) – 60 ml min^{-1}. The important information from thermal analysis is the temperature at which decomposition of organic compounds ends because it helps to determine a suitable sintering programme. The ceramic samples were sintered in the air, therefore thermal analysis was also conducted in the flow of air. Additionally, the construction of the apparatus requires the constant flow of argon as the protective gas.

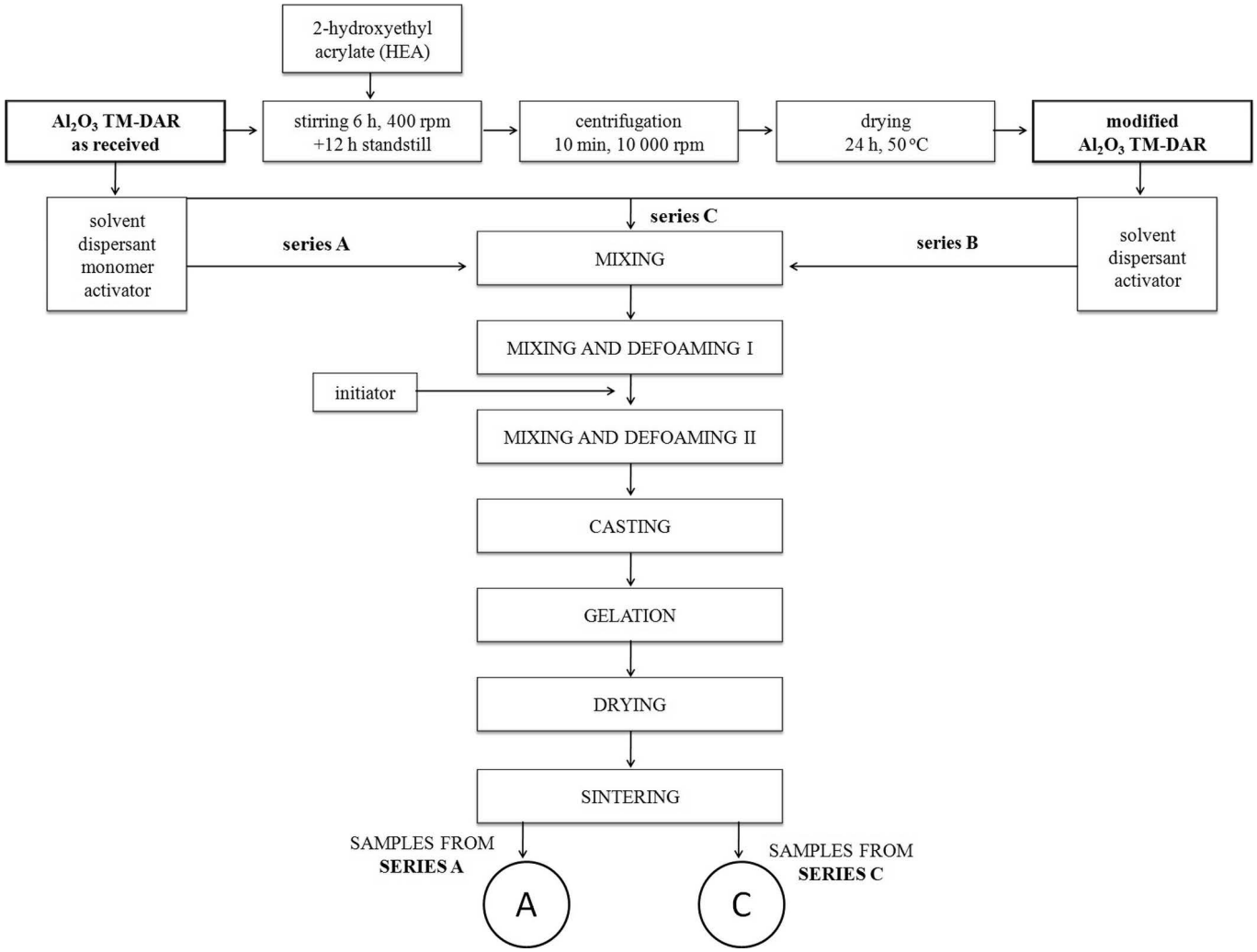

Fig. 1: Scheme showing the impregnation of Al_2O_3 powder and sample preparation applied in the research.

Table 1: Composition of the slurries used in the research.

Component	Concentration		
	Slurry A [%]	Slurry B [%]	Slurry C [%]
non-m-Al_2O_3 [a]	55	-	30
m-Al_2O_3 [a]	-	55	25
H_2O [a]	45	45	45
DAC [b]	0.3	0.3	0.3
CA [b]	0.1	0.1	0.1
HEA [b]	4	-	-
TEMED [c]	0.5	0.5	0.5
APS [c]	0.7	0.7	0.7

[a] vol%.
[b] wt% with respect to the amount of ceramic powder.
[c] wt% with the respect to the amount of monomer.

The rheological properties of slurries A and C were examined using a Kinexus Pro rotational rheometer (Malvern Instruments, UK) with a plate-plate geometry. The gap between the plates was 0.5 mm. At first, the LVER (linear viscoelastic region) at a frequency of 1 Hz was determined and then the elastic (G') and viscous (G") modules at the strain corresponding to the LVER region were plotted as a function of the frequency. The viscosities of slurries as a function of shear rate were measured in the range from 0.1 s^{-1} to 100 $s^{-1}$and then back to 0.1 s^{-1}. The densities of the green and sintered specimens were measured with the Archimedes method in kerosene and water, respectively. The tensile strength of the green bodies was calculated from the indirect tensile (Brazilian) test on a Tinius Olsen H10KS instrument with a head shift speed of 0.1 mm/min. In the Brazilian tension test, a circular disk was placed between two metallic flat plates and compressed, producing a nearly uniform tensile stress distribution normal to the loaded (vertical) diametral plane, and leading to the failure of the disk by splitting. The contact between the plates and the samples was direct without any additional support. The speed of the head shift was 0.1 mm/min. The tensile strength (σ) was calculated as $\sigma_t = (2P/\pi TD)$, where P is the force causing the damage of the sample, T and D are the thickness and the diameter of the disc-shaped sample, respectively.

A scanning electron microscope, SEM (Ultra Plus Zeiss), was used to observe the microstructure of green and sintered samples. Vickers indentations were made with a Digital Vickers Hardness Tester HVS-30T (Huatec Group Corporation, China), applying a load of 196 N. For each sample, five indentations were made. Photographs of the indentations and the measurements of the diagonals were

captured with a light microscope (Nikon Eclipse LV150N, Japan).

The measurements were performed on ten samples obtained from each slurry tested. The error was calculated as the standard deviation.

III. Results and Discussion

(1) Characteristic of modified alumina powder

The densities of non-m-Al_2O_3 and m-Al_2O_3 powders were measured with a helium pycnometer and they equalled 4.03 g/cm^3 and 3.29 g/cm^3, respectively. The density of m-Al_2O_3 is lower owing to the adsorption of the compound of lower density (d_{HEA} = 1.1 g/cm^3) on Al_2O_3 surface. The morphology of m-Al_2O_3 is presented in Fig. 2a, while Fig. 2b shows a single alumina particle with the visible lighter coating and the darker core. It may indicate the presence of adsorbed HEA on the powder surface. The thickness of the outer layer was approx. 10 nm. The powder was sputtered with carbon prior to TEM observations, therefore C was not examined by means of EDS.

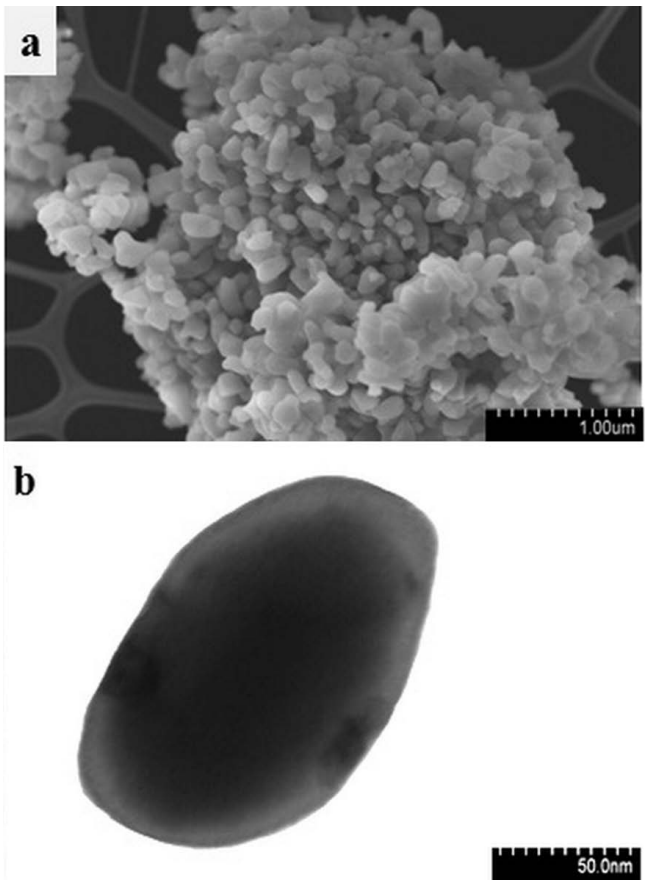

Fig. 2: TEM images of morphology of m-Al_2O_3 (a) and single particle of m-Al_2O_3 (b).

Fig. 3 shows TG, DTA, DTG curves and the data from the mass spectrometer for m-Al_2O_3 in comparison with non-m-Al_2O_3. On the basis of this measurement, the amount of HEA adsorbed on the powder surface was determined. The total mass loss was 0.44 % (according to the TG curve, Fig. 3a) in the case of non-m-Al_2O_3, which indicates a high purity of the powder and a low content of water adsorbed on the particles. For m-Al_2O_3, three stages of 2-hydroxyethyl degradation are observed. The first step up to 213 °C with the mass loss 8.42 %, the second step up to 386 °C with the mass loss 0.56 % and the third step up to the final temperature with the mass loss 0.24 %. The total mass loss for m-Al_2O_3 was 9.22 %. Fig. 3b shows more information from the mass spectrometer for m-Al_2O_3. Degradation of 2-hydroxyethyl acrylate proceeds in three steps and the main products of decomposition in the oxidizing atmosphere are H_2O and CO_2. The presence of H_2O and CO_2 are confirmed by m/z values 18 and 44, respectively. The maxima on m/z 18 and on m/z 44 at 209.6 °C and 317.9 °C are observed, which corresponds to two effects: dehydration and decomposition of hydrocarbon chain with the release of CO_2. The endothermic peak on the DTG curve with the minimum at 193 °C is visible.

(2) Properties of ceramic suspensions

Slurry B was characterized by high viscosity (too high for the gelcasting process), therefore it was not examined in terms of rheological properties. The surface of the modified powder was covered by a large number of adsorbed monomer molecules. The dispersant could not therefore act effectively in order to broaden the electric double layer around particles. As a result, the value of viscosity of the slurry from series B was not favourable for the gelcasting process.

The content of the monomer in slurries A and C has been calculated and equalled 3.21 % and 2.93 %, respectively. The amount of the monomer in both slurries is similar, therefore these slurries can be compared.

Fig. 4 shows viscoelastic features (elastic and viscous modules) as a function of the shear strain and frequency of slurries A and C. Firstly, linear viscoelastic region (LVER) at a frequency of 1 Hz for both alumina slurries was determined. The LVER was assigned at 54 % and 0.80 % shear strain respectively for suspension A(Fig. 4a) and C (Fig. 4b). For both slurries, the elastic modulus (G') predominates over the viscous modulus (G") over the whole frequency range. It follows that the elastic properties prevail in these suspensions. For slurry A (Fig. 4c), G' and G" at a frequency of 5 Hz equal 12800 Pa and 1110 Pa, respectively. For slurry C, (Fig. 4d) G' and G" at a frequency of 5 Hz equal 125 Pa and 35 Pa, respectively. For slurry A, G' and G" curves intersect at shear strain of 1.57 %. In contrast, for slurry C, the intersection of the G' and G" curves at a shear strain of 7.96 % was observed.

Fig. 5a shows the viscosity curves of slurries A and C. Viscosity values for both slurries were low and at shear rate 10 s^{-1} equalled 0.9 Pa·s and 2.4 Pa·s, respectively for A and C. Both slurries exhibited shear-thinning behaviour. These results show a similar relationship to that described by Hu *et al.*[34]. In Hu's research, modified powder also showed higher values of viscosity than pure powder. However, the differences in viscosity were small, just like in this research. Fig. 5b shows flow curves of alumina suspensions and both of them exhibit slightly thixotropic behaviour. This indicates that the internal structure of slurries is destroyed during shear and then rebuilds.

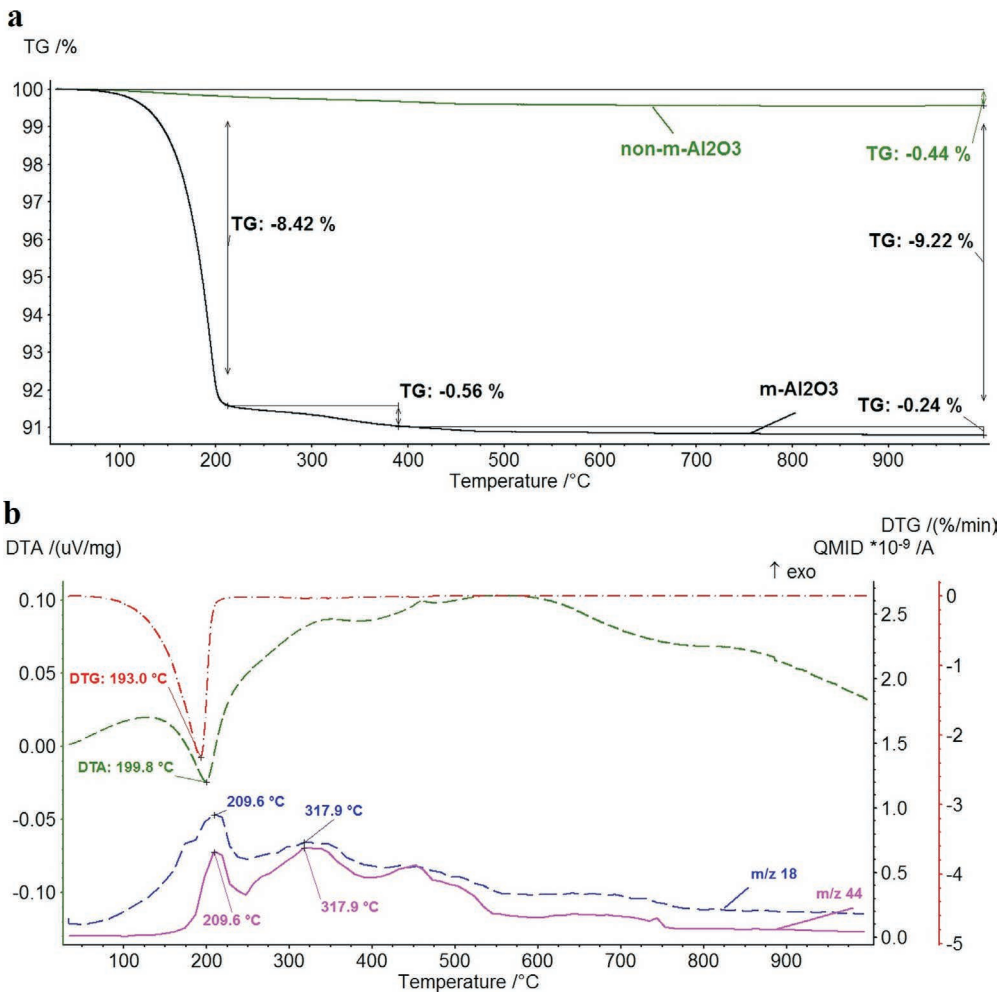

Fig. 3: a) TG curves of non-m-$Al_2O_3$and m-Al_2O_3, b) DTG/DTA/MS curves of m-Al_2O_3.

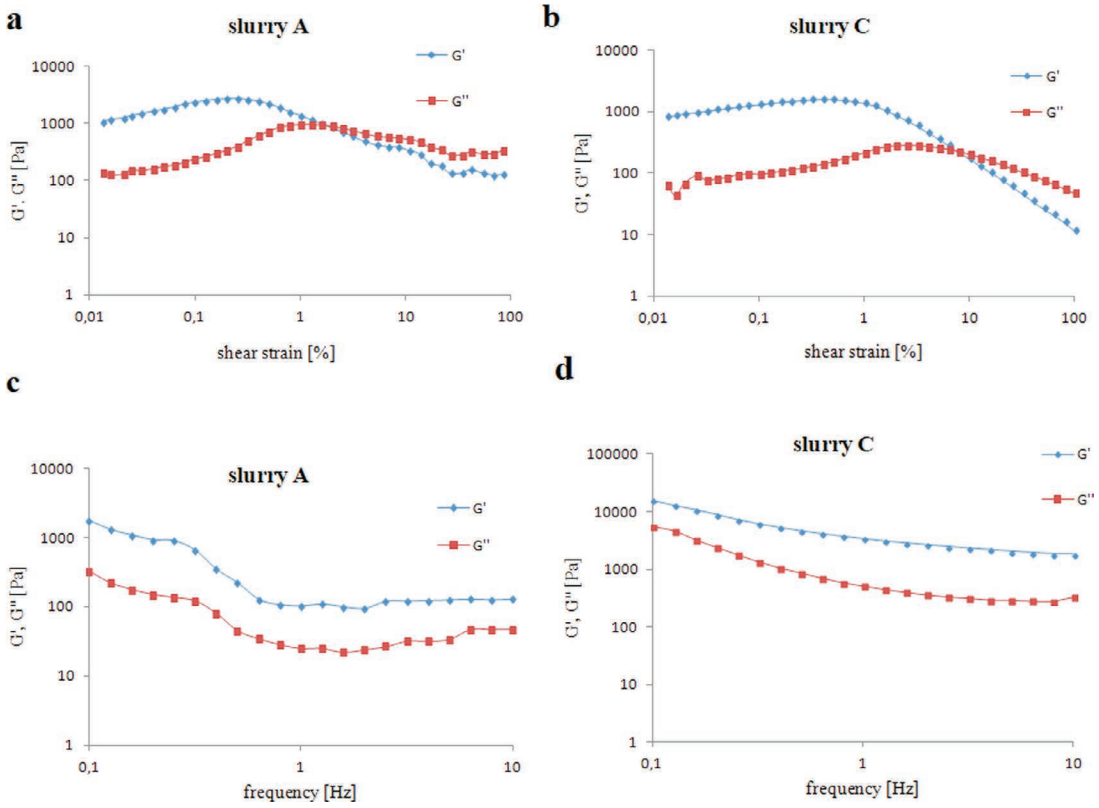

Fig. 4: Viscoelastic properties (elastic and viscous modules) as a function of shear strain and frequency of alumina slurries A (a, c) and C (b, d).

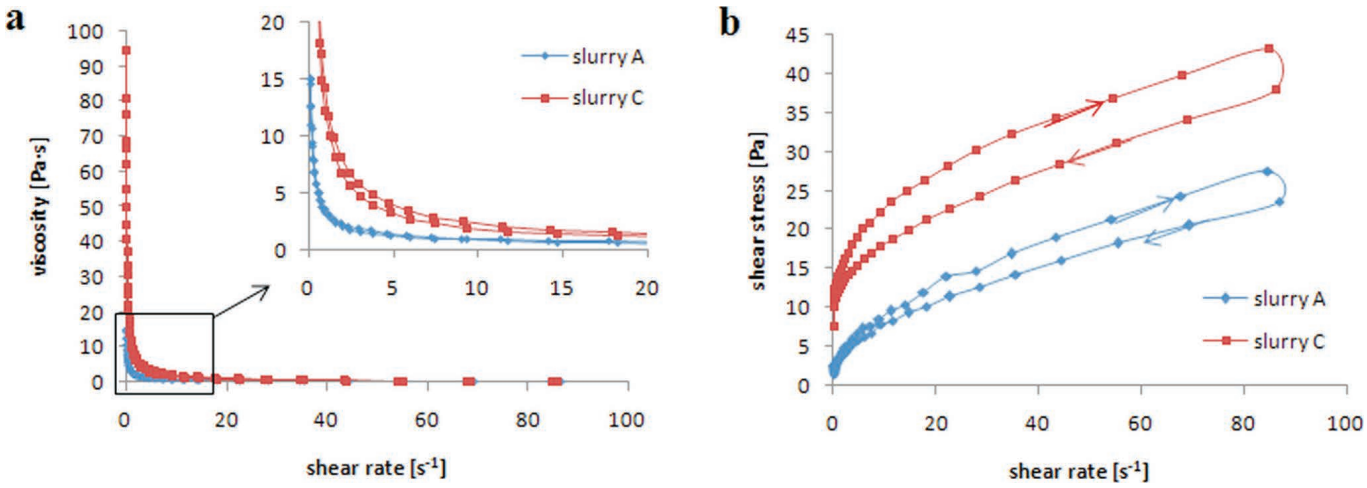

Fig. 5: Viscosity (a) and flow (b) curves of the alumina slurries A and C.

The yield stress of suspension A equals approx. 1.6 Pa. Higher yield stress (approx. 7.5 Pa) is observed for the suspension containing m-Al_2O_3.The monomer HEA is not a dispersing agent, and an excessively high quantity of this compound may cause an increase in viscosity of slurry, as it was in the case of slurry B.

(3) Sample properties

Values of selected properties for green and sintered bodies are shown in Table 2. The specimens from series C seem to have better properties than samples from series A. Relative density of green and sintered samples C equal 61 % and 98 %, respectively. In contrast, relative density of green and sintered bodies A equal 56 % and 96 %, respectively. For green bodies from series C the tensile strength is almost two times higher than for green bodies from series A(3.57 MPa and 1.83 MPa, respectively). These results are comparable with those described by Millán *et al.* However, it is worth underlining the main difference between the applied processing agents. Millán has used polysaccharides (agar, agarose and carrageenan) as gelling agents, which enables all the problems associated with radical polymerization to be avoided, but requires the use of elevated temperature. The use of modified alumina described in this paper enables gelcasting to be performed at room temperature and avoids the exfoliation of samples.

The Vickers hardness of samples with non-m-Al_2O_3 equalled 17.3 GPa. These values are comparable with the literature data described by Auerkari [35] and Cassellas [36], where the Vickers hardness of pure alumina equalled 17 – 17.5 GPa. Higher Vickers hardness was observed for the specimens containing m-Al_2O_3 and equalled 19.2 GPa.

Exfoliation of green bodies is a common problem observed in gelcasting as the result of the oxygen inhibition. Figs. 6c and 6d show green bodies after gelation. It can be observed that specimens with m-Al_2O_3 (Fig. 6d) do not exhibit any exfoliation layer. During mechanical machining of samples with the use of abrasive papers, no crushing or cracking of samples was observed. It means that polymerization has been completed properly in the whole volume of the specimen. The top part of samples containing non-m-Al_2O_3 (Fig. 6c) was exfoliated as a result of oxygen diffusion that blocked the reaction of polymerization. During mechanical machining, the samples were crushed. The explanation why m-Al_2O_3 powder prevents the negative effect of oxygen inhibition is shown schematically in Fig. 6. Fig. 6a shows slurry A and free molecules of HEA monomer which has low initial viscosity. This permits oxygen to easily diffuse into the ceramic suspension, react with the free radicals and inhibit the polymerization reaction. Fig. 6b shows slurry containing m-Al_2O_3 powder, which is characterized by shear-thinning behaviour as shown in the viscosity curve in Fig. 5. Thanks to high initial viscosity, diffusion of oxygen into the sample is blocked. This hinders reaction of the oxygen with free radicals.

Table 2: The properties of green and sintered bodies.

Series	Green bodies		Sintered bodies		
	Relative density [%]	Tensile strength [MPa]	Relative density [%]	Volumetric shrinkage [%]	Vickers hardness [GPa]
A	56.0±0.1	1.83±0.45	96.2±0.1	34.1±0.9	17.3±0.2
C	61.1±1.3	3.57±0.77	97.8±0.1	32.9±3.1	19.2±0.2

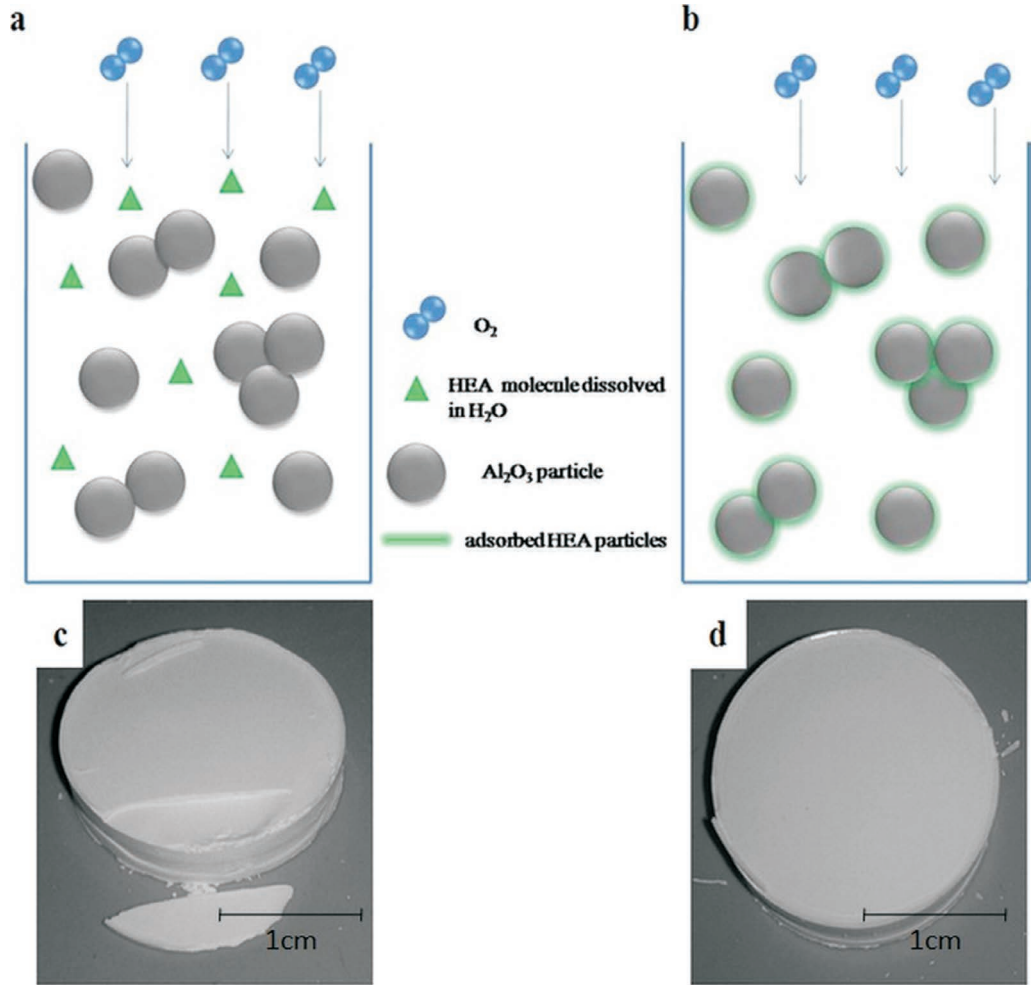

Fig. 6: The schematic explanation of oxygen inhibition phenomenon for ceramic slurries: A (a) and C (b). Images of surfaces of green bodies from series A (c) and C (d).

Fig. 7 presents SEM images of green bodies from series A and C. It allows observation of the location of the polymeric network. Photos indicate the high homogeneity of the samples. The microstructure of the two specimens looks similar. Fig. 7a and Fig. 7b show polymer in the form of bridges holding alumina particles together. For the sample containing m-Al_2O_3 (C), more polymeric bridges are visible than for the sample with non-m-Al_2O_3 (A), which is in good agreement with the results of tensile strength measurement. Additionally, coverage of Al_2O_3 particles by HEA monomer might contribute to more homogeneous distribution of the resulting polymeric binder in the whole volume of the sample. It confirms the higher value of tensile strength for these samples. Fig. 8 shows SEM images of surfaces of sintered samples (a, b). Specimens obtained from suspension based on m-Al_2O_3 (C) (Fig. 8b) have a more homogeneous and dense microstructure and are almost

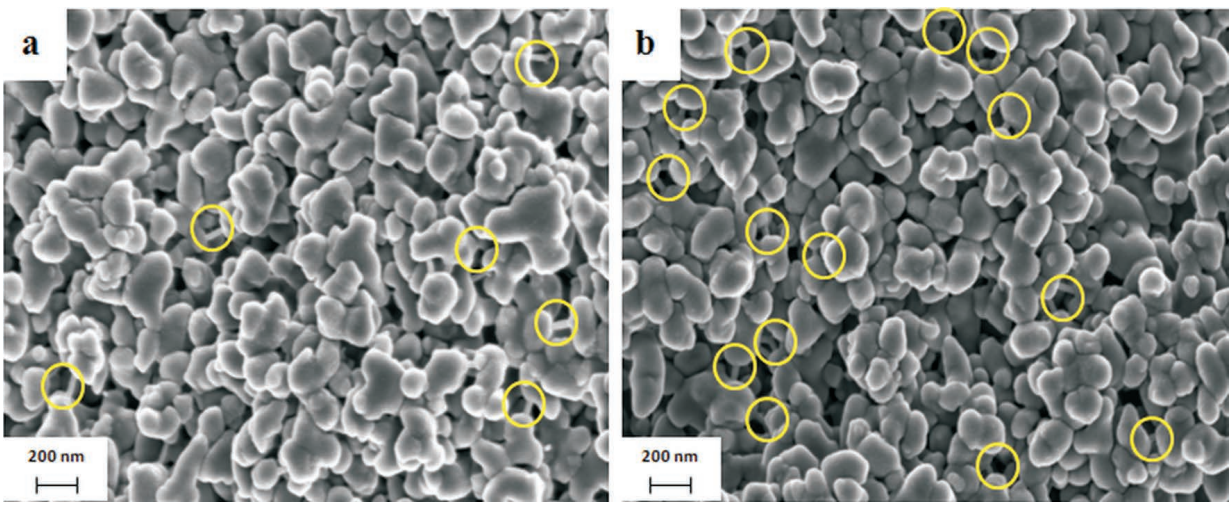

Fig. 7: SEM images of green bodies from series A (a) and C (b). Polymeric bridges are marked with yellow.

free of pores in comparison with samples based on non-m-Al_2O_3 (A) (Fig. 8a). It is also in good correlation with the measurements of the relative density of these samples (96 % and 98 % for non-m-Al_2O_3 and m-Al_2O_3, respectively). On the basis of calculations made from the presented micrographs it was found that the average grain size for samples A and C was 0.55 μm and 0.46 μm, respectively. For the sample containing non-m-Al_2O_3 (A), they were five times and for the sample containing m-Al_2O_3 (C), four times higher than the mean particle size.

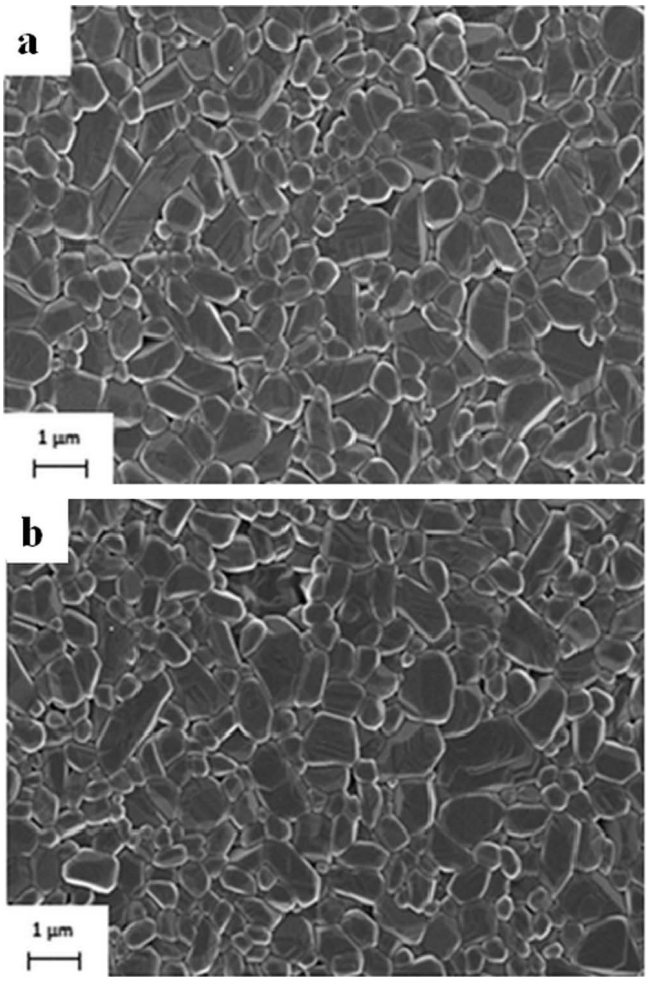

Fig. 8: SEM images of surfaces of sintered samples: (a) – based on non-modified powder (A), (b) – based on modified powder (C).

IV. Conclusions

Modification of the surface of alumina powder with commercially available monomer 2-hydroxyethyl acrylate has a favourable influence on the rheological behaviour and selected properties of green and sintered bodies. It partially solves the problem of oxygen inhibition of ceramic slurries. For slurry C, defect-free green bodies with high tensile strength without visible exfoliation were obtained. Tensile strength of samples containing m-Al_2O_3 (C) was two times higher than with non-m-Al_2O_3 (A). It may result from the more homogeneous distribution of polymeric binder in the green bodies from series C. Modified alumina powder allowed well-densified and homogeneous sintered bodies to be obtained, which was confirmed by the density measurements and the microstructure analysis with SEM. Additionally, the Vickers hardness of alumina sintered bodies was high and equalled 19.2 GPa.

Acknowledgements

This work has been financially supported by Warsaw University of Technology, Faculty of Chemistry.

References

1 Szudarska, A., Mizerski, T., Sakka, Y., Suzuki, T.S., Szafran, M.: Fabrication of textured alumina by magnetic alignment via gelcasting based on low-toxic system, *J. Eur. Ceram. Soc.,* **34**, 3841 – 3848, (2014).

2 Drdlik, D., Drdlikova, K., Hadraba, H., Maca, K.: Optical, mechanical and fractographic response of transparent alumina ceramics on erbium doping, *J. Eur. Ceram. Soc.,* **37**, 4265 – 4270, (2017).

3 Rincón, A., Chinelatto, A.S.A., Moreno, R.: Tape casting of alumina/zirconia suspension containing graphene oxide, *J. Eur. Ceram. Soc.,* **34**, 1819 – 1827, (2014).

4 López-López, E., Moreno, R., Baudin, C.: Fracture strength and fracture toughness of zirconium titanate-zirconia bulk composite materials, *J. Eur. Ceram. Soc.,* **35**, 277 – 283, (2015).

5 Hanzel, O., Sedlák, R., Sedláček, J., Bizovská, V., Bystrický, V., Girman, V., Kovalčiková, A., Dusza, J., Šajgolík, P.: Anisotropy of functional properties of SiC composites with GNPs, GO and *in situ* formed graphene, *J. Eur. Ceram. Soc.,* **37**, 3731 – 3739, (2017).

6 Al Nasiri, N., Patra, N., Ni, N., Jayaseelen, D.D., Lee, W.E.: Oxidation behaviour of SiC/SiC ceramic matrix composites in air, *J. Eur. Ceram. Soc.,* **36**, 3293 – 3302, (2016).

7 Tubío, C.R., Guitián, F., Gil, A.: Fabrication of ZnO periodic structures by 3D printing, *J. Eur. Ceram. Soc.,* **36**, 3409 – 3415, (2016)

8 Hamdelou, S., Guergouri, K.: Microstructure and electrical properties of Co-doped ZnO varistors, *J. Ceram. Sci. Technol.*, **7**, 357 – 364, (2016)

9 Wan, T., Yao, D., Yin, J., Xia, Y., Zuo, K., Liang, H., Zeng, Y.: A novel method for preparing Si_3N_4 ceramics with unidirectional oriented pores from silicon aqueous slurries, *J. Eur. Ceram. Soc.,* **37**, 3285 – 3291, (2017).

10 Rueschhoff, L.M., Trice, R.W., Youngblood, J.P.: Near-net shaping of silicon-nitride via aqueous room temperature injection molding and pressureless sintering, *Ceram. Int.*, **43**, 10791 – 10798, (2017).

11 Santacruz, I., Nieto, M.I., Binner, J., Moreno, R.: Gel casting of aqueous suspensions of $BaTiO_3$ nanopowders, *Ceram. Int.*, **35**, 321 – 326, (2009).

12 Trunec, M., Pauchly, V.: Colloidal processing of low-concentrated zirconia nano-suspension using osmotic consolidation, *Ceram. Int.*, **42**, 11838 – 11843, (2016).

13 Potoczek, M.: Gelcasting of alumina foams using agarose solutions, *Ceram. Int.*, **34**, 661 – 667, (2008).

14 Szafran, M., Wiecinska, P., Szudarska, A., Mizerski, T.: New multifunctional compounds in gelcasting process – introduction to their synthesis and application, *J. Aust. Ceram. Soc.*, **49**, 1 – 6, (2013).

15 Fan, K., Ruiz-Herrias, J., Pastor, J.Y., Gurauskis, J., Baudin, C.: Residual stress and diffraction line-broadening analysis of Al_2O_3/Y-TZP ceramic composites by neutron diffraction measurements, *Int. J. Refract. Metals. Hard. Mater.*, **64**, 122 – 134, (2017).

16 Luo, J., Eitel, R.: Aqueous tape casting of Al_2O_3 for multilayer co-fired ceramic based microfluidic chips with translucent windows, *Ceram. Int.*, **44**, 3488 – 3491, (2018).

[17] Chen, A-N., Wu, J-M., Liu, Y-X., Liu, R-Z., Cheng, L-J., Huo, W-L., Shi, Y-S., Li, C-H.: Fabrication of porous alumina ceramics by direct coagulation casting combined with 3D printing, *Ceram. Int.*, **44**, 4845 – 4852, (2018).

[18] Gauckler, L., Graule, T., Baader, F.: Ceramic forming using enzyme catalyzed reactions, *Mater. Chem. Phys*., **61**, 78 – 102, (1999).

[19] Rowthu, S., Saeidi, F., Wasmer, K., Hoffmann, P., Kuebler, J.: Flexural strength evaluations and fractography analyses of slip cast mesoporous submicron alumina, *Ceram. Int.*, **44**, 5193 – 5201, (2018).

[20] Pulgarin, H.L.C., Garrido, L.B., Albano, M.P.: Processing of different alumina-zirconia composites by slip casting, *Ceram. Int.,* **39**, 6657 – 6667, (2013).

[21] Feng, Z., Qi, J., Han, Y., Lu, T.: Deformation restraint of tape-casted transparent alumina ceramic wafers from optimized lamination, *Ceram. Int.*, **44**, 1059 – 1065, (2018).

[22] Zhang, Y., Xu, J., Qu, Y., Xi, X., Yang, J.: Gelcasting of alumina suspension using gellan gum as gelling agent, *Ceram. Int*., **40**, 5715 – 5721, (2014).

[23] Tallón, C., Yates, M., Moreno, R., Nieto, M. I.: Porosity of freeze-dried γ-Al_2O_3 powders, *Ceram. Int*., **33**, 1165 – 1169, (2007).

[24] Ligoda-Chmiel, J., Śliwa, R.E., Potoczek, M.: Flammability and acoustic absorption of alumina foam tri-functional epoxy resin composites manufactured by the infiltration process, *Compos. Part B*., **112**, 196 – 102, (2017).

[25] Montero, M., Molina, T., Szafran, M., Moreno, R., Nieto, M.I.: Alumina porous nanomaterials obtained by colloidal processing using D-fructose as dispersant and porosity promoter, *Ceram. Int*., **38**, 2779 – 2784, (2012).

[26] Falkowski, P., Bednarek, P., Danelska, A., Mizerski, T., Szafran, M.: Application of monosaccharides derivatives in colloidal processing of aluminum oxide, *J. Eur. Ceram. Soc.,* **30**, 2805 – 2811, (2010).

[27] Wiecinska, P., Graule, T., Szafran, M.: L – ascorbic acid as a new activator in fabrication of ceramics by techniques using *in situ* polymerization, *J. Eur. Ceram. Soc*., **34**, 1581 – 1589 (2014).

[28] Santacruz, I., Nieto, M.I., Moreno, R.: Alumina bodies with near-to-theoretical density by aqueous gelcasting using concentrated agarose solutions, *Ceram. Int*., **31**, 439 – 445, (2005).

[29] Gilissen, R., Erauw, J.P., Smolders, A., Vanswijgenhoven, E., Luyten, J.: Gelcasting, a near net shape technique, *Mater. Des*., **21**, 251 – 257, (2000).

[30] Studer, K., Decker, C., Beck, E., Schwalm, R.: Overcoming oxygen inhibition in UV-curing of acrylate coatings by carbon dioxide inserting, Part I, *Prog. Org. Coat*., **48**, 92 – 100, (2003).

[31] Ha, J.: Effect of atmosphere type on gelcasting behavior of Al_2O_3 and evaluation of green strength, *Ceram. Int*., **26**, 251 – 254, (2000).

[32] Pietrzak, E., Wiecińska, P., Szafran, M.: 2-carboxyethyl acrylate as a new monomer preventing negative effect of oxygen inhibition in gelcasting of alumina, *Ceram. Int*., **42**, 13682 – 13688, (2016).

[33] Zhang, S., Sha, N., Zhao, Z.: Surface modification of α-Al_2O_3 with dicarboxylic acids for the preparation of curable ceramic suspension, *J. Eur. Ceram. Soc*., **37**, 1607 – 1616, (2017).

[34] Hu, F., Liu, W., Xie, Z.: Surface modification of alumina powder particles through stearic acid for the fabrication of translucent alumina ceramics by injection molding, *Ceram. Int*., **42**, 16274 – 13280, (2016).

[35] Auerkari, P.: Mechanical and physical properties of engineering alumina ceramics, VTT Manufacturing Technology, (1996)

[36] Casellas, D., Nagl, M.M., Llanes, L., Anglada, M.: Fracture toughness of alumina and ZTA ceramics: Microstructural coarsening effects, *J. Mater. Process.*, **143 – 144**, 148 – 152, (2003).

[37] Millán, A.J., Nieto, M.I., Moreno, R., Baudin, C.: Thermogelling polysaccharides for aqueous gelcasting – Part III: mechanical and microstructural characterization of green alumina bodies, *J. Eur. Ceram. Soc.*, **22**, 2223 – 2230, (2002).